AMERICAN SOCIETY FOR MICROBIOLOGY | Antimicrobial Agents and Chemotherapy®

CLINICAL THERAPEUTICS

Interactions of Polymyxin B in Combination with Aztreonam, Minocycline, Meropenem, and Rifampin against *Escherichia coli* Producing NDM and OXA-48-Group Carbapenemases

Anna Olsson,[a] Marcus Hong,[a] Hissa Al-Farsi,[b] Christian G. Giske,[b,c] Pernilla Lagerbäck,[a] Thomas Tängdén[a]

[a]Department of Medical Sciences, Uppsala University, Uppsala, Sweden
[b]Department of Laboratory Medicine, Division of Clinical Microbiology, Karolinska Institute, Stockholm, Sweden
[c]Department of Clinical Microbiology, Karolinska University Hospital, Stockholm, Sweden

Marcus Hong and Hissa Al-Farsi contributed equally to the study; author order was based on when each joined the project.

ABSTRACT Carbapenemase-producing *Enterobacterales* pose an increasing medical threat. Combination therapy is often used for severe infections; however, there is little evidence supporting the optimal selection of drugs. This study aimed to determine the *in vitro* effects of polymyxin B combinations against carbapenemase-producing *Escherichia coli*. The interactions of polymyxin B in combination with aztreonam, meropenem, minocycline or rifampin against 20 clinical isolates of NDM and OXA-48-group-producing *E. coli* were evaluated using time-lapse microscopy; 24-h samples were spotted on plates with and without 4× MIC polymyxin B for viable counts. Whole-genome sequencing was applied to identify resistance genes and mutations. Finally, potential associations between combination effects and bacterial genotypes were assessed using Fisher's exact test. Synergistic and bactericidal effects were observed with polymyxin B and minocycline against 11/20 strains and with polymyxin B and rifampin against 9/20 strains. The combinations of polymyxin B and aztreonam or meropenem showed synergy against 2/20 strains. Negligible resistance development against polymyxin B was detected. Synergy with polymyxin B and minocycline was associated with genes involved in efflux (presence of *tet[B]*, wild-type *soxR*, and the *marB* mutation H44Q) and lipopolysaccharide synthesis (*eptA* C27Y, *lpxB* mutations, and *lpxK* L323S). Synergy with polymyxin B and rifampin was associated with sequence variations in *arnT*, which plays a role in lipid A modification. Polymyxin B in combination with minocycline or rifampin frequently showed positive interactions against NDM- and OXA-48-group-producing *E. coli*. Synergy was associated with genes encoding efflux and components of the bacterial outer membrane.

KEYWORDS carbapenem resistance, Gram-negative bacteria, combination therapy, synergy, polymyxins

The increasing prevalence of carbapenemase-producing *Enterobacterales* is an emerging threat worldwide. These bacteria are common causes of severe infections, such as sepsis, urinary tract infections, and hospital-acquired pneumonia, and are difficult to treat due to their multidrug-resistant phenotypes (1–3). The last resort antibiotics polymyxin B and E (colistin) remain active against most isolates and have been widely used for these infections (4, 5). Although combination therapy is always recommended based on observational clinical data (6), evidence is still scarce on the optimal selection of companion drug.

In vitro synergy against carbapenemase-producing *Enterobacterales* has been shown with polymyxins in combination with multiple other antibiotics (e.g., β-lactams, minocycline, rifampin) (7–10). Most studies have addressed *Klebsiella pneumoniae*, and data are

Citation Olsson A, Hong M, Al-Farsi H, Giske CG, Lagerbäck P, Tängdén T. 2021. Interactions of polymyxin B in combination with aztreonam, minocycline, meropenem, and rifampin against *Escherichia coli* producing NDM and OXA-48-group carbapenemases. Antimicrob Agents Chemother 65:e01065-21. https://doi.org/10.1128/AAC.01065-21.

Address correspondence to Thomas Tängdén, thomas.tangden@medsci.uu.se.

Received 25 May 2021
Returned for modification 30 June 2021
Accepted 1 September 2021
Accepted manuscript posted online 13 September 2021
Published 17 November 2021

TABLE 1 MIC values (mg/liter) and classification of antibiotic susceptibilities according to CLSI breakpoint tables M100-ED30:2020[a]

		Polymyxins	β-lactams		Tetracyclines	Rifamycins
Strain	Carbapenemase	PMB	ATM	MEM	MIN	RIF
ARU770	NDM-1	0.5 (I)	>16 (R)	>64 (R)	32 (R)	16 (NA)
ARU771	NDM-1	0.5 (I)	>16 (R)	64 (R)	32 (R)	16 (NA)
ARU772	NDM-7	0.5 (I)	>16 (R)	32 (R)	4 (S)	16 (NA)
ARU773	NDM-5	0.5 (I)	1 (S)	64 (R)	16 (R)	16 (NA)
ARU774	NDM-1	0.5 (I)	>16 (R)	>64 (R)	16 (R)	32 (NA)
ARU775	NDM-5	0.5 (I)	>16 (R)	>64 (R)	4 (S)	16 (NA)
ARU776	NDM-1	0.5 (I)	>16 (R)	>64 (R)	4 (S)	16 (NA)
ARU777	NDM-5	0.5 (I)	>16 (R)	16 (R)	16 (R)	16 (NA)
ARU778	NDM-1	0.5 (I)	>16 (R)	16 (R)	16 (R)	32 (NA)
ARU779	NDM-5	0.5 (I)	>16 (R)	>64 (R)	8 (I)	16 (NA)
ARU780	NDM-5	0.5 (I)	8 (I)	64 (R)	8 (I)	16 (NA)
ARU781	NDM-5	0.5 (I)	>16 (R)	>64 (R)	8 (I)	16 (NA)
ARU782	NDM-5	0.5 (I)	>16 (R)	64 (R)	4 (S)	32 (NA)
ARU783	OXA-48	0.5 (I)	≤0.5 (S)	0.5 (S)	2 (S)	8 (NA)
ARU785	OXA-48	0.5 (I)	>16 (R)	2 (S)	1 (S)	8 (NA)
ARU786	OXA-48	0.5 (I)	≤0.5 (S)	1 (S)	8 (I)	16 (NA)
ARU787	OXA-181	0.5 (I)	>16 (R)	1 (S)	8 (I)	32 (NA)
ARU788	OXA-181	0.5 (I)	>16 (R)	0.5 (S)	16 (R)	16 (NA)
ARU790	NDM-5, OXA-181	0.5 (I)	>16 (R)	16 (R)	32 (R)	32 (NA)
ARU791	NDM-1, OXA-48	0.5 (I)	>16 (R)	32 (R)	64 (R)	32 (NA)

[a]Abbreviations: S, susceptible; I, intermediate; R, resistant; NA, not available; ATM, aztreonam; MEM, meropenem; MIN, minocycline; PMB, polymyxin B; RIF, rifampin

limited for *Escherichia coli*. The prevailing theory for the observed synergistic interactions is that the polymyxin-induced membrane disruption increases the membrane permeability, thereby facilitating entry of the second antibiotic (11, 12). Polymyxins may also act by counteracting the function of membrane-associated efflux pumps (11). However, the mechanisms of synergistic interaction remain largely unknown. Therefore, to date, the activity of antibiotic combinations cannot be predicted based on antibiotic susceptibility testing of single drugs or genetic characterization.

We previously evaluated automated time-lapse microscopy (the oCelloScope, BioSense Solutions Aps, Farum, Denmark) as a screening tool for antibiotic combinations (13) and reported synergy with several polymyxin B combinations against multidrug-resistant *K. pneumoniae* and *Pseudomonas aeruginosa* (9, 14). In the present study, we evaluated the effects of polymyxin B in combination with aztreonam, meropenem, minocycline and rifampin against 20 NDM- and OXA-48-producing *E. coli* in 24-h time-lapse microscopy experiments. A spot assay in which 24-h samples were placed on plates with and without polymyxin B at 4× MIC was added to provide viability data and detect emerging subpopulations with reduced susceptibility. All isolates were subjected to whole-genome sequencing to map genes known to impact the susceptibility to the tested antibiotics. Finally, we explored potential associations between the observed combination effects and bacterial genetics.

RESULTS

Antibiotic susceptibilities. All strains were intermediate to polymyxin B with MICs of 0.5 mg/liter (Table 1). Only three strains were susceptible to aztreonam. Strains carrying bla_{NDM} (bla_{NDM-1}, bla_{NDM-5} and bla_{NDM-7}) were resistant to meropenem, whereas those carrying only bla_{OXA-48} –group carbapenemase genes (bla_{OXA-48} and $bla_{OXA-181}$) were classified as susceptible. Minocycline MICs varied greatly between the strains (range 1–64 mg/liter) and rifampin MICs were mostly high (8 to 32 mg/liter).

Resistance genes and mutations. Polymyxin resistance genes *mcr-1 – 10* were not found in the strains. All strains harbored genes encoding carbapenemases: NDM (n = 13), OXA-48-group enzymes (n = 5) or both (n =2) (Table 2). In addition, other β-lactamase genes were present in all strains, most frequently bla_{TEM-1B} (n = 15), $bla_{CTX-M-15}$ (n = 14) and bla_{OXA-1} (n = 11). Tetracycline efflux genes *tet(A)* (n = 8), *tet(B)* (n = 8) or *tet(D)* (n = 2) were found in 18/20 strains. All eight strains harboring *tet(B)* and eight of nine strains with wild type *soxR* (Table 3) had increased minocycline MICs (≥8 mg/liter). An amino acid

TABLE 2 Identified resistance genes and amino acid variations[a]

Antibiotic class	Resistance gene	Strain																			
		ARU770	ARU771	ARU772	ARU773	ARU774	ARU775	ARU776	ARU777	ARU778	ARU779	ARU780	ARU781	ARU782	ARU783	ARU785	ARU786	ARU787	ARU788	ARU790	ARU791
β-lactams	bla_{CMY-2}											+							+	+	
	bla_{CMY-6}									+											
	bla_{CMY-42}							+								+		+			
	$bla_{CTX-M-15}$	+	+	+		+	+	+	+				+	+		+		+	+	+	+
	bla_{NDM-1}	+	+			+		+		+											+
	bla_{NDM-5}				+		+		+		+	+	+	+						+	
	bla_{NDM-7}			+																	
	bla_{OXA-1}			+		+	+	+	+	+			+	+				+	+	+	
	bla_{OXA-9}	+																			
	bla_{OXA-48}														+	+	+				+
	$bla_{OXA-181}$																	+	+	+	
	bla_{TEM-1B}	†	+		+	+	+	+		+	†	+	+	+	+		+	+	+	+	+
Tetracyclines	*tet(A)*			+		+	+	+					+	+	+			+			
	tet(B)	+	+		+				+	+	+								+	+	
	tet(D)																+				+
Rifamycins	*rpoB*[b]	+	+	+	+	+	+	+	+	+	+	+	+	+	+	+	+	+	+	G1261C	+

[a]Abbreviations: +, full-length gene present and without amino acid variations compared to the reference in the ResFinder database; †, gene sequence not complete due to scaffold or contig-breaks after assembly.
[b]*Escherichia coli* K12 MG1655 used as reference (NCBI accession number: NC_000913.3).

TABLE 3 Genetic differences[a] in genes encoding porins, efflux pumps, and their regulators

Porin, efflux pump or regulator	Function	Gene	Strain									
			ARU770	**ARU771**	**ARU772**	**ARU773**	**ARU774**	**ARU775**	**ARU776**	**ARU777**	**ARU778**	**ARU779**
OmpC	S	*ompC*[b]	Q54K N165D G216A I218V	Q54K N165D G216A I218V	L296V	Q54K N165D G216A I218V	Q54K N165D G216A I218V	Q54K N165D G216A I218V	Q54K N165D G216A I218V		G216A I218V	Q54K N165D G216A I218V
OmpF	S	*ompF*[b]	N31fs	N31fs								Y112F F118I Y204F A233fs
AcrAB-To1C	S	*acrA*									T104A[d] A167S[d]	T104A[d]
	S	*acrB*									H596N[d]	H596N[d]
	R	*acrR*	T5N[c]	T5N[c]			V29fs	V29fs	V29fs			K80fs
	S	*tolC*								Y120H		
marRAB operon	R	*marR*	G103S[d] Y137H[d]	G103S[d] Y137H[d]	G103S[d] Y137H[d]	G103S[d] Y137H[d]					S3N[d] G103S[d] Y137H[d]	†
	A	*marA*					†			†	S127N	
	R	*marB*	H44Q	H44Q	H44Q	H44Q				X	S5L A10T A33G H44Q	S5L L12F A17T V20I H44Q
SoxSR	A	*soxS*										
	A	*soxR*					A111T[d]	A111T[d]	A111T[d]	A111T[d]	G74R[d]	T38S[d] G74R[d]
RobA	A	*rob*									Q20H A171S	
OmpR-EnvZ	A	*ompR*										
	A	*EnvZ*									A25V T466A	A25V T466A
			ARU780	**ARU781**	**ARU782**	**ARU783**	**ARU785**	**ARU786**	**ARU787**	**ARU788**	**ARU790**	**ARU791**
OmpC	S	*ompC*[b]	G216A I218V	L296V	Q54K N165D G216A I218V	M57V G216A I218V L296V	Q54K N165D G216A I218V	Q54K N165D G216A I218V	Q54K N165D G216A I218V	L296V	L296V	G216A I218V L296V
OmpF	S	*ompF*[b]					Y112F F118I Y204F	Y112F F118I Y204F				S199fs
AcrAB-TolC	S	*acrA*				T104A[d] N221Y[d]	T104A[d]	T104A[d]				
	S	*acrB*				H596N[d]	H596N[d]	H596N[d]				K1036T
	R	*acrR*	S87*	S68*	V29fs				V29fs			V43fs
	S	*tolC*				A440T						

(Continued on next page)

TABLE 3 (Continued)

Porin, efflux pump or regulator	Function	Gene	Strain									
marRAB operon	R	*marR*	A70E	G103S[d]		G103S[d]	K62R[d]	K62R[d]		G103S[d]	†	X
			G103S[d]	Y137H[d]		Y137H[d]	Δ97-107	G103S[d]		Y137H[d]		
			Y137H[d]				Y137H[d]	Y137H[d]				
	A	*marA*										
	R	*marB*	H44Q	S5L		S5L	S5L	S5L		H44Q	H44Q	H44Q
				T24P		A17T	L12F	L12F				
				A33G		V20I	A17T	A17T				
				V38A		H44Q	V20I	V20I				
				H44Q			H44Q	H44Q				
SoxSR	A	*soxS*										A12S[c]
	A	*soxR*			A111T[d]	T38S[d]	T38S[d]	T38S[d]	A111T[d]			
						G74R[d]	G74R[d]	G74R[d]				
RobA	A	*rob*										
OmpR-EnvZ	A	*ompR*										
	A	*EnvZ*				A25V	A25V	A25V				
						T466A	T466A	T466A				

[a]*Escherichia coli* K12 MG1655 (NCBI accession number: NC_000913.3) used as reference. Abbreviations: A, activator; R, repressor; S, subunit; X, gene not found; *, stop codon; fs, frameshift; †, gene sequence not complete due to scaffold or contig-breaks after assembly.

[b]Only amino acid variations in β-strand-encoding regions of *ompC* and *ompF* are shown.

[c]Mutations previously known to cause increased resistance.

[d]Mutation not previously associated with increased efflux.

substitution in *rpoB* (G1261C) was identified in ARU790 but was not located in any region known to cause resistance to rifampin (15).

Eleven strains had a sequence variation (T5N, $n = 2$), frameshift ($n = 7$) or a premature stop codon ($n = 2$) in *acrR* (Table 3). These genetic variations likely result in increased expression of the AcrAB-TolC efflux pump (16), for which aztreonam, meropenem, minocycline and rifampin are known substrates (17–19). A mutation in the AcrAB-TolC efflux regulatory gene *soxS* (A12S), previously reported to be associated with resistance, was found in one strain (20). We identified additional mutations commonly encountered in clinical isolates but have not been shown to increase AcrAB-TolC efflux activity alone: *acrA* (T104A, A167S and N221Y [21]), *marR*, (S3N, K62R, G103S and Y137H) and *soxR* (A111T, T38S and G74R) (22). Several other mutations with unknown effects were found in *marB*; the most frequent mutation was H44Q which was found in 14/20 strains. In 19/20 strains, genes encoding the OmpC and OmpF porins, that facilitate entry of β-lactams (3), were associated with sequence variations in the β-sheet regions composing the porin channels (23, 24) (Table 3). Several amino acid variations were identified in genes encoding enzymes involved in the synthesis or modification of LPS, mainly in *lpxB*, *lpxK*, *lpxH, arnT*, and *eptA* (25) (Table 4). Moreover, there was large variability in core oligosaccharide types, as determined based on the *waa* locus (25, 26); R1 was most frequent ($n = 8$), followed by R4 ($n = 5$), R2 ($n = 4$) and R3 ($n = 3$).

Time-lapse microscopy experiments. The most effective combination was polymyxin B and minocycline, showing a positive interaction against 11/20 strains (Fig. 1), closely followed by polymyxin B and rifampin with 9/20 strains. For polymyxin B and meropenem a positive interaction was seen against 3/20 strains. The combination of polymyxin B and aztreonam was not superior to monotherapy at any of the tested concentrations when using the predefined cutoffs for bacterial growth (BCA >8 at 24 h and $SESA_{max} > 5.8$). Negative interaction by the combination in comparison to monotherapy was observed with polymyxin B in combinations with meropenem (ARU770, ARU779, ARU781 and ARU788) and aztreonam (ARU788).

Spot assay. The spot assay showed synergistic and bactericidal effects with 22/23 combinations that indicated positive interactions in the time-lapse microscopy experiments (Fig. 1). In addition, synergistic and bactericidal effects were detected with polymyxin B and aztreonam against two strains (ARU780 and ARU786). No antibiotic carryover effect was observed (data not shown). Growth on polymyxin B at 4× MIC after 24 h was detected for 267 of the 504 spots (53%) that grew on nonantibiotic-containing plates (Fig. 1). However, in all but three cases, growth on 4× MIC polymyxin B was only 2 $\log_{10}$ CFU/ml (= the lower limit of detection, LOD) and repeated susceptibility testing of 67 spots revealed no increase in polymyxin B MICs indicating an inoculum effect (data not shown).

Associations between combination effects and bacterial genetics. Statistical analysis using Fisher's exact text showed that synergy with polymyxin B and minocycline was significantly associated with the tetracycline efflux gene *tet(B)*; synergy was noted in 7/8 strains carrying this gene ($P = 0.0281$) (Table S1). In contrast, a negative association was found for *tet(A)*; synergy was only observed in 1/8 harboring this gene ($P = 0.0045$). Statistically significant associations were also found when comparing wild type to any mutation(s) in *marB* ($P = 0.0081$), *marR* ($P = 0.0499$) and *soxR* ($P = 0.0098$), which are all involved in AcrAB-TolC efflux. On the mutation level, the *marB* mutation H44Q was frequently associated with a synergistic effect (10/11, $P = 0.04985$) (Table S2). No specific *marR* mutation was significantly associated with synergy. Reduced susceptibility to minocycline in strains carrying *tet(B)* ($n = 8$) or wild type *soxR* ($n = 9$) was reversed in the presence of polymyxin B in 7 and 8 cases, respectively (Fig. 1C). In contrast, the *soxR* mutation A111T was negatively associated with synergy (1/11, $P = 0.0499$). Moreover, sequence alterations in the *lpxB* ($P = 0.0499$) and *lpxK* ($P = 0.0499$) genes, encoding enzymes involved in lipid A synthesis, were associated with synergy (Table S3) (25). On the mutation level, the *lpxK* mutation L323S ($P = 0.0499$) was present in 10/11 strains against which synergy was found, whereas the *eptA* mutation C27Y showed a negative association (1/11, $P = 0.0499$).

TABLE 4 Genetic differences[a] in genes encoding enzymes involved in lipopolysaccharide synthesis and core oligosaccharide type

Function	Gene	Strain																			
		ARU770	ARU771	ARU772	ARU773	ARU774	ARU775	ARU776	ARU777	ARU778	ARU779	ARU780	ARU781	ARU782	ARU783	ARU785	ARU786	ARU787	ARU788	ARU790	ARU791
Structural component	*lpp*										R77H										
Enzymes catalyzing lipid A synthesis	*lpxA*																				
	lpxC																				
	lpxD									R206C I224V	I224V				K147R I224V	K147R I224V	K147R I224V				
	lpxH	K58Q	K58Q	K58Q T139M W190G	K58Q T139M					V13A R57H K58Q P210T	V13A K58Q	K58Q			V13A K58Q	V13A K58Q R109Q	V13A K58Q		K58Q T139M W190G	K58Q T139M W190G	K58Q
	lpxB	E3K	E3K	E3K H32R	H32R V93I					H32R A180G H189Y E247A	H32R A180G L256M M260L	R220C	H32R A180G H189Y		H32R K84T A180G L256M	H32R A180G H189Y L256M	H32R A180G H189Y L256M		E3K H32R	E3K H32R	H32R
	lpxK	A278T L323S	A278T L323S	L323S	Y93N A278T L323S					D118G T319A L323S N328H	T319A L323S	L323S	Q74K L323S		D118G D225E T319A L323S	V66I D118G R293L A294P E298G T319A L323S	V66I D118G R293L A294P E298G T319A L323S		L323S	L323S	L323S
	lpxL									M254I											M185T
	lpxM	†								A98V											
Core oligosacharide type	-	R3	R3	R1	R4	R1	R2	R1	R2	R1	R4	R1	R1	R2	R4	R4	R4	R2	R1	R1	R3
Regulators of lpxC	*ftsH*																				
	lapB														T201A D323N E331K	T201A T366A	T201A T366A				†
Modifies lipid A	*arnT*	T116A T197S N232D L248M V261L T281A S322P P408S D522N	T116A T197S N232D L248M V261L T281A S322P P408S D522N		T116A T197S N232D L248M V261L T281A S322P P408S D522N				T116A T197S N232D L248M V261L T281A S322P P408S D522N	T33M D108N N232D V261L T281A S322P A535V	T116A T197S N232D L248M V261L T281A S322P P408S D522N		T116A T197M N232D V261L T281A		T116A N232D V261L T281A S322P P408S	T116A T197S N232D L248M V261L T281A S322P P408S D522N	T116A T197S N232D L248M V261L T281A S322P P408S D522N				N232D
	eptA	D348G T413S	D348G T413S	D348G T413S	D348G T413S	C27Y	C27Y	C27Y	C27Y	L14F A15S A21T I26V A39V S69G A106T Q123R F130L L137I A147T V163I L211S V217I E232G A332V D348G E366D K414Q	A147T D348G	E547K	E547K	C27Y	D348G	K233T D348G	K233T D348G	C27Y	D348G T413S	D348G T413S	V320Del VLWND NDGGC KGACD RVPHQ NVTAL NLPDQ CIN T413S
	pagP									S11F L82Q T117I	N2I R35G A39T				L82Q	K5Q L82Q	K5Q L82Q				L82Q
	lpxP				†		G125F		Q4K F253Y T263A	A46T F253Y E73K G187S F253Y	Q4K T263A				M47I F253Y T263A	Q4K F253Y T263A	G192S F253Y T263A				

[a]*Escherichia coli* K-12 MG1655 (NCBI accession number: NC_000913.3) used as reference. Abbreviations: Del, deletion; †, gene sequence not complete due to scaffold or contig-breaks after assembly.

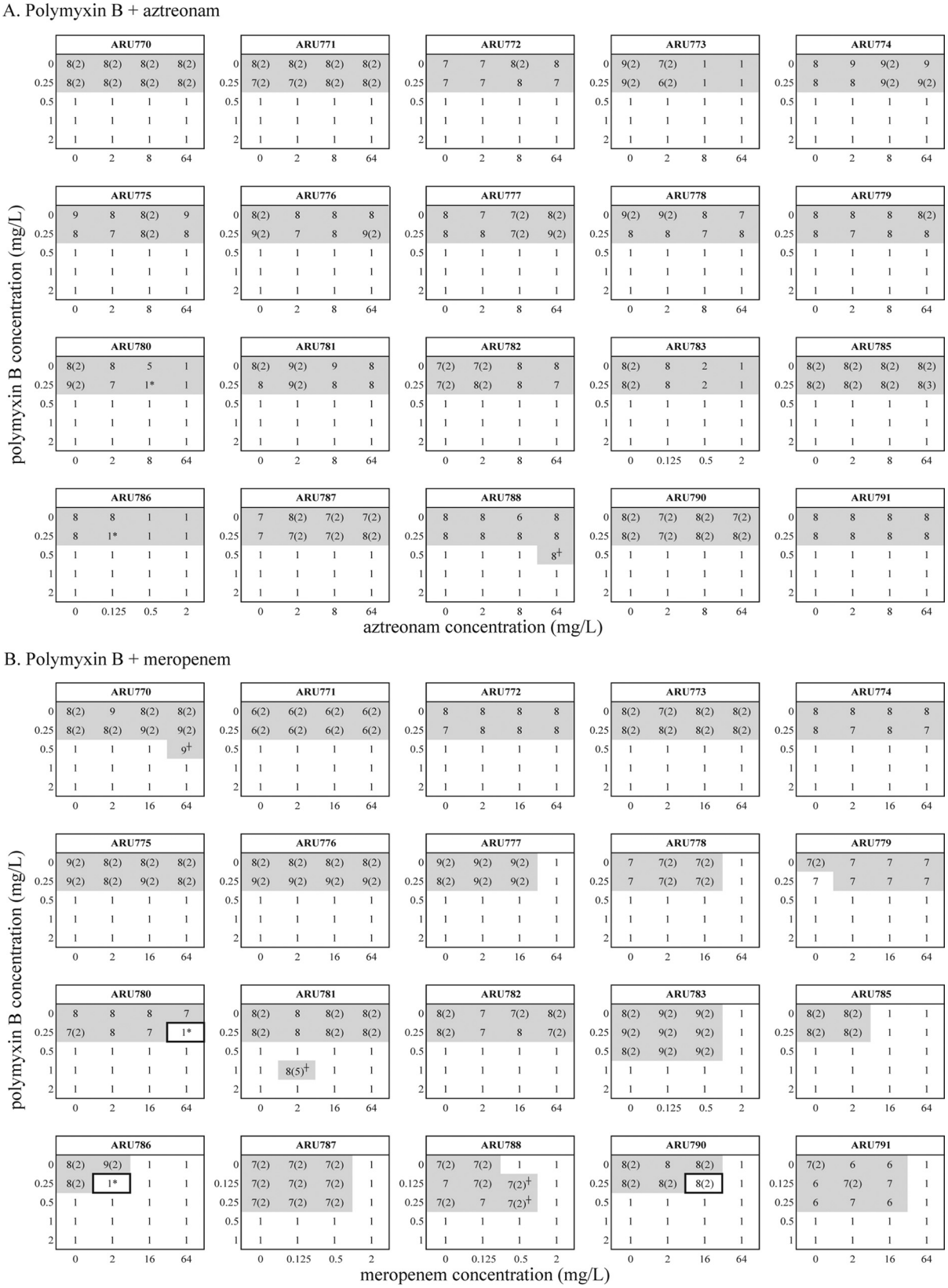

FIG 1 Results of time-lapse microscopy experiments and spot assay. For time-lapse microscopy experiments, wells with BCA >8 and $SESA_{max}$ >5.8, indicating a bacterial density of $>10^6$ CFU/ml at 24 h, are highlighted in gray and combinations showing positive interactions in the time-lapse microscopy experiments are marked with a square. For spot assay, bacterial growth on MH-II plates at 24 h is presented in $\log_{10}$ CFU/ml and no visible growth is set to 1 $\log_{10}$ CFU/ml (LOD = 2 $\log_{10}$ CFU/ml). Growth on 4× MIC polymyxin B is presented in parentheses. Synergistic and bactericidal effect with the combination, as determined with the spot assay, is highlighted with "*" and antagonistic effect "+."

C. Polymyxin B + minocycline

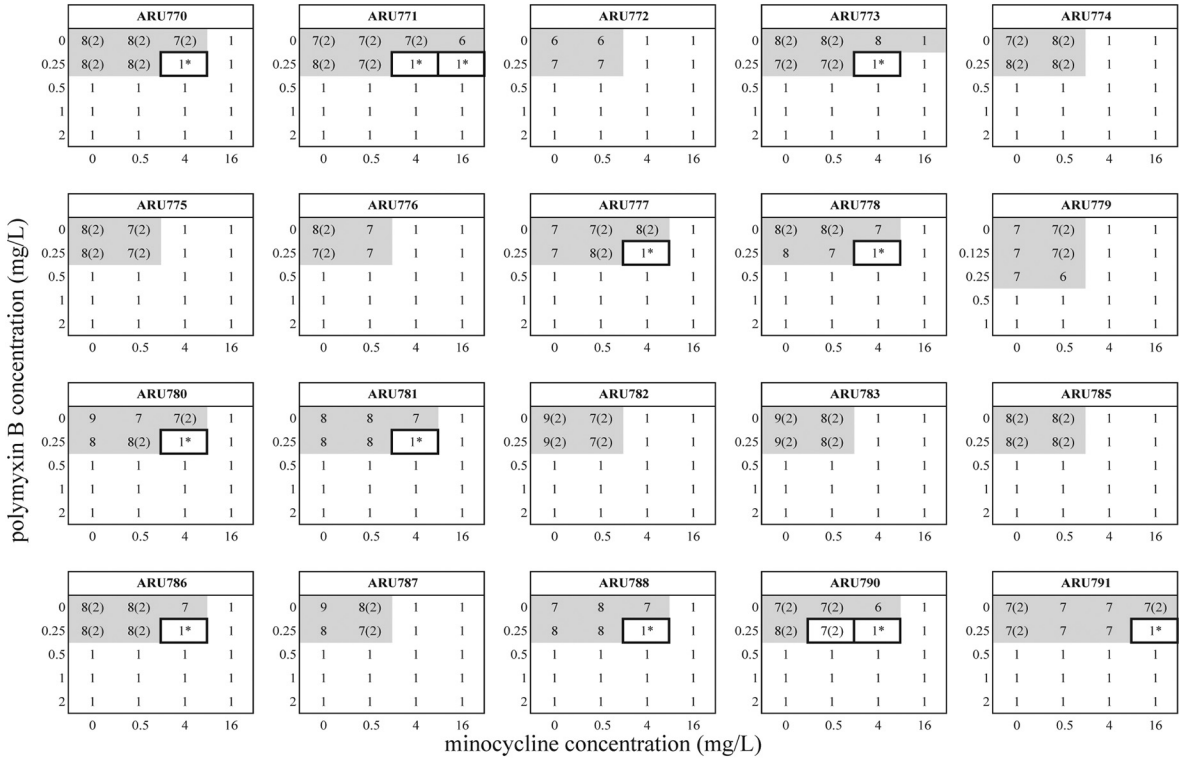

D. Polymyxin B + rifampicin

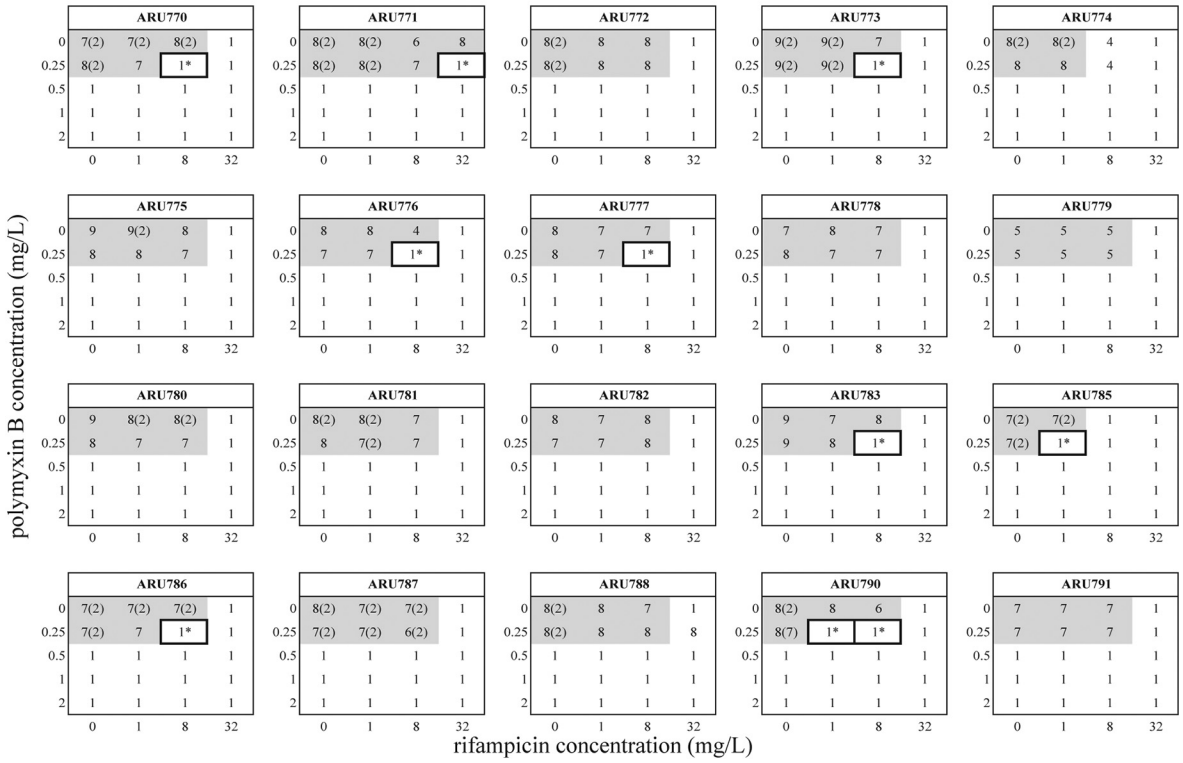

FIG 1 (Continued)

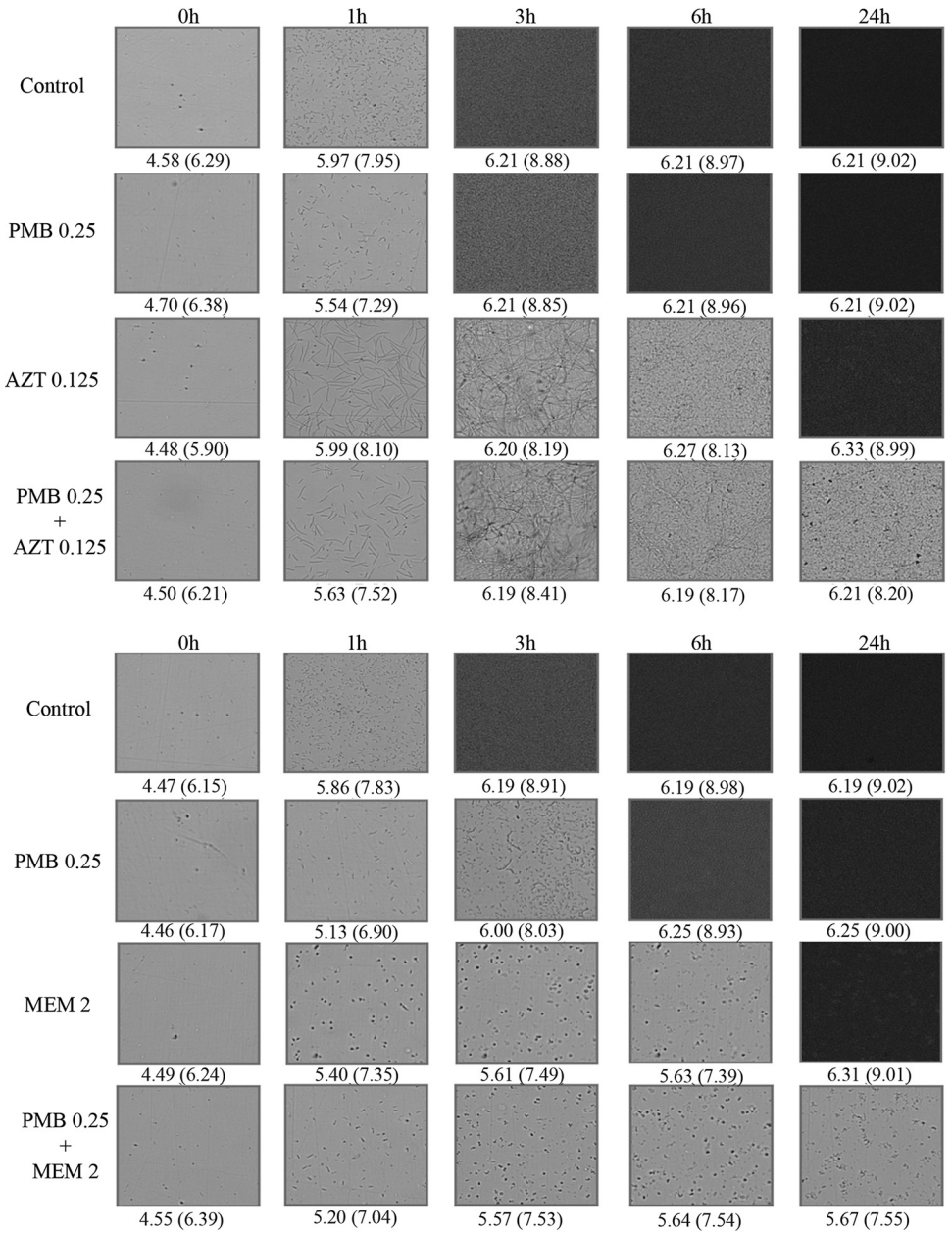

FIG 2 Changes in cell morphology during exposure to polymyxin B (PMB), aztreonam (ATM) and meropenem (MEM) against NDM-producing *Escherichia coli* ARU786. Antibiotics were added to the indicated concentrations (mg/liter). Images were obtained at 0, 1, 3, 6 and 24 h. The $SESA_{max}$ and BCA (in parentheses) values are presented below each image. Filamentation during exposure to aztreonam alone resulted in high BCA and $SESA_{max}$ values despite low viable counts.

No significant associations were noted for the polymyxin B and rifampin combination for genes encoding efflux, porin loss or enzymatic resistance. However, several mutations in the *arnT* gene encoding a lipid A-modifying enzyme were positively associated with synergy (*P values* ranging from 0.005 to 0.022) (Table S4). Because synergy was rarely observed with polymyxin B and aztreonam or meropenem, statistical analyses were not considered meaningful for these combinations.

DISCUSSION

In this study, positive interactions were frequently found with polymyxin B combined with minocycline or rifampin against NDM- and OXA-48-group producing *E. coli*.

In contrast, according to the 24-h viable count data, combinations of polymyxin B and aztreonam or meropenem showed synergy and a bactericidal activity only against 2/20 strains. Negligible resistance development against polymyxin B was identified with all combinations. Although growth on polymyxin B at 4× MIC was often observed following antibiotic exposure, bacterial concentrations were typically low ($\leq$2 $\log_{10}$ CFU/ml) and no MIC elevations were detected. Therefore, we deduce that this observation likely reflects an inoculum effect, which is of uncertain clinical relevance, rather than emergence or selection of resistant subpopulations.

Importantly, nonsusceptibility to one or both constituent antibiotics does not preclude a synergistic activity when combining the two drugs. Polymyxin B and minocycline performed well in this study despite that all strains were intermediate to polymyxin B, and most were intermediate or resistant to minocycline. To our knowledge, data on the activity of this combination against *Enterobacterales* are scarce. However, polymyxin B was previously reported to induce 8-fold reductions in minocycline MICs in *mcr-1* positive *E. coli* and *K. pneumoniae* (8). Also, we recently reported synergy with this combination in time-kill experiments against 4/5 *K. pneumoniae* producing NDM, KPC or OXA-48 enzymes, including strains displaying phenotypic resistance to one or both drugs (9).

Gram-negative bacteria are intrinsically resistant to rifampin due to the inability of this molecule to penetrate the bacterial outer membrane. Yet, polymyxin B and rifampin showed synergy against 9/20 strains in this study. Our results are consistent with other studies reporting positive interactions with polymyxins and rifampin. One study observed a bactericidal activity with polymyxin B and rifampin against 2/5 KPC-producing *E. coli* (10) and we previously reported synergy with this combination against 4/5 NDM-, KPC- or OXA-48-producing *K. pneumoniae* (9). Another study showed synergy with this combination against NDM- and MCR-1-producing polymyxin-resistant *E. coli* (7).

Our results indicate polymyxin B and meropenem has low synergistic potential against NDM- and OXA-48-producing *E. coli*. Polymyxin-carbapenem combinations have been widely recommended for severe infections caused by carbapenemase-producing *Enterobacterales* (4, 6). Observational clinical data support the use of such combinations against KPC-producing *K. pneumoniae* with carbapenem MICs $\leq$8 mg/liter (4, 5). However, their efficacy against *E. coli* and strains producing non-KPC enzymes remains uncertain as illustrated in this study. As new β-lactam/β-lactamase inhibitor combinations become available, it is important to consider the bacterial genetic determinants and strain-dependent differences in antibiotic susceptibility to the single drugs and combinations. While meropenem-vaborbactam and imipenem-relebactam are normally active against KPC-producing isolates (6), their use will be limited in areas where other carbapenemases are predominant. Aztreonam is highly intriguing in this context due to its stability to metallo-β-lactamases, such as NDM-1. Still, polymyxin B and aztreonam failed to show positive interactions against most of the tested strains in this study. To our knowledge, previous data on this combination is lacking for *E. coli* and is scarce for *K. pneumoniae* (9, 27). Clearly, coadministration of polymyxin B was generally not sufficient to circumvent enzymatic resistance in these strains, e.g., mediated by CTX-M-15, which was produced by 14/20 strains and has high affinity for aztreonam (2, 28).

We observed several biologically plausible and statistically significant associations between the interactions of polymyxin B and minocycline and bacterial genetics. For example, synergy was positively associated with genes involved in efflux, which can be counteracted by the membrane-disrupting activity of polymyxin B. Statistically significant associations were observed for mutant *marB* and *marR*. These genes regulate AcrAB-TolC efflux, for which minocycline and multiple antibiotics (e.g., meropenem, aztreonam and rifampin) are known substrates. The association with the *marB* mutation H44Q likely results from reduced repression of *marA*, which in turn increases AcrAB-TolC activity (1) (Table S2). While wild type *soxR* was positively associated with reduced susceptibility to minocycline and a synergistic activity with the combination, a negative association was found for *soxR* mutation A111T. This observation aligns with

a previous study where this mutation was not associated with resistance to tetracycline or other antibiotics (22).

Further, several sequence variations in genes involved in LPS synthesis or modification showed statistically significant associations with enhanced activity of polymyxin B and minocycline or rifampin in combination (25). These genetic variations might have altered minocycline or rifampin permeability as well as polymyxin B targets. For the minocycline combination, mutant *lpxB* and *lpxK* L323S were associated with synergy, while the C27Y mutation in *eptA* was negatively associated with synergy. LpxB has a role in the addition of a saccharide to the lipid A structure and LpxK catalyzes the addition of the phosphate group. The cation-linkages between phosphates of the lipid A molecules are an important feature for membrane stability and the negatively charged phosphate groups are also a target of polymyxin B (12). Interestingly, minocycline has a potent antioxidant activity and can also directly chelate Ca^{2+} which could also contribute to synergy with polymyxins by displacing the cation-linkages (Ca^{2+} and Mg^{2+}) between two lipid A molecules and increase permeability (12, 29). Synergy with polymyxin B and rifampin was positively associated with mutations in *arnT*. Both ArnT and EptA mediate additions of positively charged moieties to the phosphate groups, which could alter polymyxin B activity (25).

The spot assay added information on CFU/ml reductions and enabled assessment of resistance development during antibiotic exposure. The measurement of bacterial concentrations with this assay is similar to standard time-kill experiments but has lower resolution as individual colonies are not counted (only growth/no growth with a 1:10 dilution between spots) and a higher LOD of 2 $\log_{10}$ versus 1 $\log_{10}$ CFU/ml. Also, the time-lapse microscopy method differs from time-kill experiments in that there is no shaking during incubation and the total volume is lower (200 μl versus ca 2 ml) (13). The agreement in results between the oCelloScope readout and spot assay was excellent with the exception of aztreonam, for which filamentation complicates readout using the available SESA and BCA algorithms (Fig. 2). Filament formation is associated with β-lactam antibiotics targeting penicillin-binding protein 3 (PBP3), including aztreonam, and was previously observed in time-lapse microscopy experiments with *K. pneumoniae* and *P. aeruginosa* (9, 13, 14).

The extensive genetic characterization of resistance mechanisms and mutations, and the assessment of their potential associations with the combination effects is a strength of this study. However, we recognize that more research is needed to validate our findings and determine causality. Combination therapy will remain important in the treatment of multidrug-resistant pathogens to enhance bacterial killing and suppress emergence of resistance, and further efforts to better understand the determinants of synergistic interactions are needed. A range of clinically achievable drug concentrations was used to reduce the risk of overlooking synergistic activity. However, in some cases positive interactions were detected only at the highest drug concentrations, which may be associated with a risk of toxicity in patients. As always, translation of *in vitro* findings to the clinical setting must also be made with caution due to the absence of an immune system and other biological processes as well as differences in growth conditions.

In conclusion, we report positive interactions with polymyxin B combinations against *E. coli* producing NDM and OXA-48-group carbapenemases, most frequently with minocycline or rifampin. These combinations should be further explored *in vitro* and *in vivo* to determine their therapeutic potential. Resistance genes or mutations involved in efflux, LPS synthesis or modification and lipid A modification were associated with synergistic effect. Deciphering such associations between combination effects and bacterial genetics is a first step toward understanding the mechanisms of synergistic interactions, and may help inform individualized therapy tailored to the infecting pathogen in future patients.

MATERIALS AND METHODS

Antibiotics and media. All antibiotics were purchased from Sigma-Aldrich (St. Louis, MO). Stock solutions of 10,000 mg/liter were prepared by dissolving polymyxin B and meropenem in sterile water and

aztreonam, minocycline and rifampin in DMSO. Cation-adjusted Mueller-Hinton (MH-II) (BD Diagnostics, Sparks, MD, USA) broth and agar plates were used for all experiments.

Strains and antibiotic susceptibility testing. Twenty carbapenemase-producing *E. coli* isolates collected from hospitalized patients in Oman during 2015 were used. The susceptibilities to polymyxin B, meropenem, minocycline. and rifampin were tested with broth microdilution according to CLSI recommendations (30). Aztreonam MICs were determined using the Sensititre Antimicrobial Susceptibility Testing System (Trek Diagnostic Systems, Cleveland, OH) according to the manufacturer's instructions. Susceptibilities were interpreted using CLSI clinical breakpoints M100-ED30:2020 (31).

Genetic characterization. DNA was extracted with the MagNA Pure96 System (F. Hoffmann-La Roche, Basel, Switzerland) followed by whole-genome sequencing using HiSeq 2500 (Illumina, San Diego, USA). *De novo* assembly was accomplished using CLC Genomics Workbench (version 20). ResFinder 4.1 was employed to identify acquired resistance genes, (32). Because all strains were susceptible, the search for polymyxin B resistance genes was restricted to *mcr*. To identify variations in genes involved in AcrAB-TolC efflux (*acrA*, *acrB*, *acrR*, *tolC*, *marR*, *marA*, *marB*, *soxS*, *soxR*, *rob)*, porin-specific entry (*ompC*, *ompF*, *ompR*, *envZ*), LPS synthesis (*lpp*, *lpxA-D*, *lpxH*, *lpxK-M*, *lpxP*, *ftsH*, *lapB*, *arnT*, *eptA*, *pagP* and the *waa* locus) and rifampin resistance (*rpoB*) genes were aligned against *E. coli* MG1655 K-12 (NCBI Reference Sequence: NC_000913.3) and the core oligosaccharide type was determined based on the *waa* locus composition (25).

Time-lapse microscopy. Screening was performed using the oCelloScope instrument as previously described (9, 13, 14). Briefly, bacteria in exponential growth phase were added to achieve starting inocula $\sim 10^6$ CFU/ml and a total volume of 200 μl per well in a flat-bottom 96-well microtiter plate (Greiner Bio-One GmbH, Frickenhausen, Germany). The following clinically achievable drug concentrations were used: polymyxin B, 0.25, 0.5, 1 and 2 mg/liter; aztreonam, 2, 8 and 64 mg/liter; meropenem, 2, 16 and 64 mg/liter; minocycline, 0.5, 4 and 16 mg/liter; and rifampin, 1, 8 and 32 mg/liter. If one of the single antibiotics of a combination prevented bacterial growth at all these concentrations, a lower concentration range was used: polymyxin B, 0.125, 0.25, 0.5 and 1 mg/liter; aztreonam, 0.125, 0.5 and 2 mg/liter; and meropenem, 0.125, 0.5 and 2 mg/liter. Quality control strains (*E. coli* ATCC 25922 for polymyxin B, aztreonam and meropenem and *Staphylococcus aureus* ATCC 29213 for minocycline and rifampin) were included in all experiments. The 96-well microtiter plate was incubated at 37°C and images of each well were generated every 15 min for 24 h by the oCelloScope. Focus was set using the bottom search function, illumination level was set to 150, and image distance to 4.9 μm.

The Background Corrected Absorption (BCA) and Segmentation Extracted Surface Area (SESA) algorithms of the UniExplorer software version 6.0.0 (Philips BioCell A/S, Allerød, Denmark) were used to determine bacterial density. The LOD was $\sim 1 \times 10^4$ CFU/ml. A BCA value >8 and a maximum SESA value ($SESA_{max}$) >5.8 were used as cutoff values to indicate a bacterial density of $>10^6$ CFU/ml at 24 h (13). The combination was considered to exhibit a positive interaction if BCA and $SESA_{max}$ were below these cutoffs with the combination but not with any of the constituent single antibiotics at the same concentration. Conversely, the combination was considered to show a negative interaction if BCA and $SESA_{max}$ were above the cutoff values with the combination but not with the single antibiotics at the same drug concentrations.

Spot assay and population analysis. After completing the 24-h time-lapse microscopy experiments, samples from each well were serially diluted in PBS and 10 μl aliquots were spotted on MH-II agar plates with and without 2 mg/liter polymyxin B (4× MIC) (33). Bacterial growth was recorded after overnight incubation at 37°C. The LOD was 2 $\log_{10}$ CFU/ml. No visible bacterial growth was recorded as 1 $\log_{10}$ CFU/ml in the analysis of synergistic and bactericidal effects. Synergy was defined as $\geq$2-$\log_{10}$ CFU/ml reduction in bacterial concentrations with the combination at 24 h compared with the most potent single antibiotic (33). A bactericidal effect was defined as $\geq$ 3-$\log_{10}$ reduction in CFU/ml at 24 h compared with the starting inoculum. A $\geq$1-$\log_{10}$ CFU/ml increase in bacterial concentrations with the combination compared to one or both single antibiotics at the same drug concentration was classified as antagonism. Potential antibiotic carryover effects were assessed by regular plating of 100 μl undiluted and 10-fold diluted samples, allowing the sample to sink in before spreading. Two strains producing NDM-1 (ARU770) or OXA-48 (ARU783) were randomly selected for MIC determination of all spots growing on 4× MIC plates after 24 h.

Statistical analyses. Potential associations between synergistic effects with an antibiotic combination and the presence of resistance genes and mutations in the tested strains were assessed by Fisher's exact test using R (version 3.6.3). Resistance genes showing statistically significant associations, defined as $P < 0.05$, were further explored to identify correlations between combination interactions and specific mutations in these genes.

Data availability. Whole-genome sequencing raw data (reads) were deposited in the Sequence Read Archive (SRA) as project PRJNA544438 (accession numbers SRR9113453, SRR9113455-SRR9113460, SRR9113462, SRR9113468, SRR9113469, SRR9113478-SRR9113487).

SUPPLEMENTAL MATERIAL

Supplemental material is available online only.

SUPPLEMENTAL FILE 1, PDF file, 1 MB.

ACKNOWLEDGMENTS

This study was funded by the Joint Programming Initiative on Antimicrobial Resistance (JPIAMR), grant no. 2015-06825 (T.T.); AFA Insurance, grant no. 180124 (T.T.); and the Swedish Research Council, grant no. 2019-05911 and 2020-02320 (T.T.).

We thank Karin Vickberg for excellent technical assistance.

REFERENCES

1. Li X-Z, Plésiat P, Nikaido H. 2015. The challenge of efflux-mediated antibiotic resistance in Gram-negative bacteria. Clin Microbiol Rev 28:337–418. https://doi.org/10.1128/CMR.00117-14.
2. Tooke CL, Hinchliffe P, Bragginton EC, Colenso CK, Hirvonen VHA, Takebayashi Y, Spencer J. 2019. β-Lactamases and β-lactamase inhibitors in the 21st century. J Mol Biol 431:3472–3500. https://doi.org/10.1016/j.jmb.2019.04.002.
3. Choi U, Lee C-R. 2019. Distinct roles of outer membrane porins in antibiotic resistance and membrane integrity in Escherichia coli. Front Microbiol 10:953. https://doi.org/10.3389/fmicb.2019.00953.
4. Tsuji BT, Pogue JM, Zavascki AP, Paul M, Daikos GL, Forrest A, Giacobbe DR, Viscoli C, Giamarellou H, Karaiskos I, Kaye D, Mouton JW, Tam VH, Thamlikitkul V, Wunderink RG, Li J, Nation RL, Kaye KS. 2019. International Consensus Guidelines for the Optimal Use of the Polymyxins: endorsed by the American College of Clinical Pharmacy (ACCP), European Society of Clinical Microbiology and Infectious Diseases (ESCMID), Infectious Diseases Society of America (IDSA), International Society for Anti-infective Pharmacology (ISAP), Society of Critical Care Medicine (SCCM), and Society of Infectious Diseases Pharmacists (SIDP). Pharmacotherapy 39:10–39. https://doi.org/10.1002/phar.2209.
5. Paul M, Daikos GL, Durante-Mangoni E, Yahav D, Carmeli Y, Benattar YD, Skiada A, Andini R, Eliakim-Raz N, Nutman A, Zusman O, Antoniadou A, Pafundi PC, Adler A, Dickstein Y, Pavleas I, Zampino R, Daitch V, Bitterman R, Zayyad H, Koppel F, Levi I, Babich T, Friberg LE, Mouton JW, Theuretzbacher U, Leibovici L. 2018. Colistin alone versus colistin plus meropenem for treatment of severe infections caused by carbapenem-resistant Gram-negative bacteria: an open-label, randomised controlled trial. Lancet Infect Dis 18:391–400. https://doi.org/10.1016/S1473-3099(18)30099-9.
6. Infectious Diseases Society of America. 2020. Infectious Diseases Society of America antimicrobial resistant treatment guidance: Gram-negative bacterial infections. 2020.
7. Yu Y, Walsh TR, Yang R-S, Zheng M, Wei M-C, Tyrrell JM, Wang Y, Liao X-P, Sun J, Liu Y-H. 2019. Novel partners with colistin to increase its in vivo therapeutic effectiveness and prevent the occurrence of colistin resistance in NDM- and MCR-co-producing Escherichia coli in a murine infection model. J Antimicrob Chemother 74:87–95.
8. MacNair CR, Stokes JM, Carfrae LA, Fiebig-Comyn AA, Coombes BK, Mulvey MR, Brown ED. 2018. Overcoming mcr-1 mediated colistin resistance with colistin in combination with other antibiotics. Nat Commun 9:458–458. https://doi.org/10.1038/s41467-018-02875-z.
9. Wistrand-Yuen P, Olsson A, Skarp K-P, Friberg LE, Nielsen EI, Lagerbäck P, Tängdén T. 2020. Evaluation of polymyxin B in combination with 13 other antibiotics against carbapenemase-producing Klebsiella pneumoniae in time-lapse microscopy and time-kill experiments. Clin Microbiol Infect 26:1214–1221. https://doi.org/10.1016/j.cmi.2020.03.007.
10. Urban C, Mariano N, Rahal JJ. 2010. In vitro double and triple bactericidal activities of Doripenem, Polymyxin B, and Rifampin against multidrug-resistant Acinetobacter baumannii, Pseudomonas aeruginosa, Klebsiella pneumoniae, and Escherichia coli. Antimicrob Agents Chemother 54:2732–2734. https://doi.org/10.1128/AAC.01768-09.
11. Bowers DR, Cao H, Zhou J, Ledesma KR, Sun D, Lomovskaya O, Tam VH. 2015. Assessment of Minocycline and Polymyxin B combination against Acinetobacter baumannii. Antimicrob Agents Chemother 59:2720–2725. https://doi.org/10.1128/AAC.04110-14.
12. Li J, Nation RL, Kaye KS. 2019. Polymyxin Antibiotics: from Laboratory Bench to Bedside, Advances in Experimental Medicine and Biology 1145. Springer Nature Switzerland AG.
13. Ungphakorn W, Lagerbäck P, Nielsen EI, Tängdén T. 2018. Automated time-lapse microscopy a novel method for screening of antibiotic combination effects against multidrug-resistant Gram-negative bacteria. Clin Microbiol Infect 24:778.e7-778–e14. https://doi.org/10.1016/j.cmi.2017.10.029.
14. Olsson A, Wistrand-Yuen P, Nielsen EI, Friberg LE, Sandegren L, Lagerbäck P, Tängdén T. 2020. Evaluation of the efficacy of antibiotic combinations against multidrug-resistant Pseudomonas aeruginosa in automated time-lapse microscopy and static time-kill experiments. Antimicrob Agents Chemother https://doi.org/10.1128/AAC.02111-19.
15. Wu EY, Hilliker AK. 2017. Identification of Rifampicin resistance mutations in Escherichia coli, including an unusual deletion mutation. MMB 27:356–362.
16. Lee JO, Cho K-S, Kim OB. 2014. Overproduction of AcrR increases organic solvent tolerance mediated by modulation of SoxS regulon in Escherichia coli. Appl Microbiol Biotechnol 98:8763–8773. https://doi.org/10.1007/s00253-014-6024-9.
17. Nakashima R, Sakurai K, Yamasaki S, Nishino K, Yamaguchi A. 2011. Structures of the multidrug exporter AcrB reveal a proximal multisite drug-binding pocket. Nature 480:565–569. https://doi.org/10.1038/nature10641.
18. Chetri S, Bhowmik D, Paul D, Pandey P, Chanda DD, Chakravarty A, Bora D, Bhattacharjee A. 2019. AcrAB-TolC efflux pump system plays a role in carbapenem non-susceptibility in Escherichia coli. BMC Microbiol 19:210. https://doi.org/10.1186/s12866-019-1589-1.
19. Elkins CA, Nikaido H. 2002. Substrate specificity of the RND-type multidrug efflux pumps AcrB and AcrD of Escherichia coli is determined predominately by two large periplasmic loops. J Bacteriol 184:6490–6498. https://doi.org/10.1128/JB.184.23.6490-6499.2002.
20. Aly SA, Boothe DM, Suh S-J. 2015. A novel alanine to serine substitution mutation in SoxS induces overexpression of efflux pumps and contributes to multidrug resistance in clinical Escherichia coli isolates. J Antimicrob Chemother 70:2228–2233. https://doi.org/10.1093/jac/dkv105.
21. Elkins CA, Mullis LB, Lacher DW, Jung CM. 2010. Single nucleotide polymorphism analysis of the major tripartite multidrug efflux pump of Escherichia coli: functional conservation in disparate animal reservoirs despite exposure to antimicrobial chemotherapy. Antimicrob Agents Chemother 54:1007–1015. https://doi.org/10.1128/AAC.01126-09.
22. Vinué L, Hooper DC, Jacoby GA. 2018. Chromosomal mutations that accompany qnr in clinical isolates of Escherichia coli. Int J Antimicrob Agents 51:479–483. https://doi.org/10.1016/j.ijantimicag.2018.01.012.
23. Baslé A, Rummel G, Storici P, Rosenbusch JP, Schirmer T. 2006. Crystal structure of osmoporin OmpC from E. coli at 2.0 A. J Mol Biol 362:933–942. https://doi.org/10.1016/j.jmb.2006.08.002.
24. Nikaido H. 2003. Molecular basis of bacterial outer membrane permeability revisited. Microbiol Mol Biol Rev 67:593–656. https://doi.org/10.1128/MMBR.67.4.593-656.2003.
25. Bertani B, Ruiz N. 2018. Function and biogenesis of lipopolysaccharides. EcoSal Plus 8 https://doi.org/10.1128/ecosalplus.ESP-0001-2018.
26. Amor K, Heinrichs DE, Frirdich E, Ziebell K, Johnson RP, Whitfield C. 2000. Distribution of core oligosaccharide types in lipopolysaccharides from Escherichia coli. Infect Immun 68:1116–1124. https://doi.org/10.1128/IAI.68.3.1116-1124.2000.
27. Tängdén T, Hickman RA, Forsberg P, Lagerbäck P, Giske CG, Cars O. 2014. Evaluation of double- and triple-antibiotic combinations for VIM- and NDM-producing klebsiella pneumoniae by in vitro time-kill experiments. Antimicrob Agents Chemother 58:1757–1762. https://doi.org/10.1128/AAC.00741-13.
28. Lohans CT, Brem J, Schofield CJ. 2017. New Delhi Metallo-β-Lactamase 1 catalyzes Avibactam and Aztreonam hydrolysis. Antimicrob Agents Chemother 61 https://doi.org/10.1128/AAC.01224-17.
29. Dai C, Ciccotosto GD, Cappai R, Wang Y, Tang S, Xiao X, Velkov T. 2017. Minocycline attenuates colistin-induced neurotoxicity via suppression of apoptosis, mitochondrial dysfunction and oxidative stress. J Antimicrob Chemother 72:1635–1645. https://doi.org/10.1093/jac/dkx037.
30. Clinical and Laboratory Standards Institute. 2018. M07-A11 Methods for dilution antimicrobial susceptibility tests for bacteria that grow aerobically; approved standard—11th ed
31. Clinical and Laboratory Standards Institute. 2020. M100-ED30:2020Performance Standards for Antimicrobial Susceptibility Testing, 30th Edition.
32. Bortolaia V, Kaas RS, Ruppe E, Roberts MC, Schwarz S, Cattoir V, Philippon A, Allesoe RL, Rebelo AR, Florensa AF, Fagelhauer L, Chakraborty T, Neumann B, Werner G, Bender JK, Stingl K, Nguyen M, Coppens J, Xavier BB, Malhotra-Kumar S, Westh H, Pinholt M, Anjum MF, Duggett NA, Kempf I, Nykäsenoja S, Olkkola S, Wieczorek K, Amaro A, Clemente L, Mossong J, Losch S, Ragimbeau C, Lund O, Aarestrup FM. 2020. ResFinder 4.0 for predictions of phenotypes from genotypes. J Antimicrob Chemother 75:3491–3500. https://doi.org/10.1093/jac/dkaa345.
33. Clinical and Laboratory Standards Institute. 1999. M26-ED01:1999. Methods for Determining Bactericidal Activity of Antimicrobial Agents, 1st Edition